Hydrol. Earth Syst. Sci. Discuss., 11, 11533–11563, 2014
www.hydrol-earth-syst-sci-discuss.net/11/11533/2014/
doi:10.5194/hessd-11-11533-2014

Hydrology and Earth System Sciences
Open Access
Discussions

Identifying water mass depletion in Northern Iraq observed by GRACE

G. Mulder[1], T. N. Olsthoorn[1], D. A. M. A. Al-Manmi[2], E. J. O. Schrama[1], and E. H. Smidt[1]

[1]Delft University of Technology, Delft, the Netherlands
[2]University of Sulaimani, Department of Geology, Sulaymaniyah, Iraq

Received: 3 September 2014 – Accepted: 21 September 2014 – Published: 17 October 2014

Correspondence to: G. Mulder (gert.mulder@gmail.com)

Published by Copernicus Publications on behalf of the European Geosciences Union.

Abstract

Observations acquired by Gravity Recovery And Climate Experiment (GRACE) mission indicate a mass loss of $31 \pm 3\,km^3$ or $130 \pm 14\,mm$ in Northern Iraq between 2007 and 2009. This data is used as an independent validation of a hydrologic model of the region including lake mass variations. We developed a rainfall–runoff model for five tributaries of the Tigris River, based on local geology and climate conditions. Model inputs are precipitation from Tropical Rainfall Measurement Mission (TRMM) observations, and potential evaporation from GLDAS model parameters. Our model includes a representation of the karstified aquifers that cause large natural groundwater variations in this region. Observed river discharges were used to calibrate our model. In order to get the total mass variations, we corrected for lake mass variations derived from Moderate Resolution Imaging Spectroradiometer (MODIS) in combination with satellite altimetry and some in-situ data. Our rainfall–runoff model confirms that Northern Iraq suffered a drought between 2007 and 2009 and is consistent with the mass loss observed by GRACE over that period. Also, GRACE observed the annual cycle predicted by the rainfall–runoff model. The total mass depletion seen by GRACE between 2007 and 2009 is mainly explained by a lake mass depletion of $74 \pm 4\,mm$ and a natural groundwater depletion of $37 \pm 6\,mm$. Our findings indicate that man-made groundwater extraction has a minor influence in this region while depletion of lake mass and geology play a key role.

1 Introduction

During 2007 till 2009, Northern Iraq suffered a severe drought, with rainfall rates 40 % below normal levels based on both satellite (Trigo et al., 2010) and local rainfall measurements (Fadhil, 2011). In the same period, discharge of large springs and rivers decreased substantially and data from the GRACE satellite mission indicated a permanent loss of water mass in the region (UN-ESCWA and BGR, 2013; Voss et al.,

HESSD
11, 11533–11563, 2014

2013). Decrease in rainfall and water availability directly affected the water supply of towns and villages (Michel et al., 2012) and caused a strong decline in crop yields in Northern Iraq (Trigo et al., 2010). About 100 000 people have left their homes in Northern Iraq as a consequence of depleted water sources (McLeman, 2011). From 2009 onwards, rainfall rates have been rising, but are still lower than before the drought period, which is in line with the decrease in rainfall in the region predicted by (Gibelin and Déqué, 2003; Giorgi and Lionello, 2008; Mariotti et al., 2008).

Concurrent with decreasing water availability in the region, water demands are fast increasing during the last years due to population growth and increase of irrigated agriculture (Altinbilek, 2004; Beaumont, 1998). Especially in Turkey, water demands increase rapidly due to the Southeastern Anatolia Project (GAP), which includes the construction of dams and irrigation schemes in the upstream Tigris catchment. At this moment, about 42 000 ha of this irrigation scheme is operational, with 53 400 ha under development and another 500 000 ha is planned in future years (Altinbilek, 1997). Additionally, several dams and irrigations projects are under construction in the Iranian headwaters of the Tigris, which will reduce river flows in Northern Iraq permanently (Ali, 2007).

This means that especially Northern Iraq has to cope with a permanent decrease of its water resources over the last years due to lower rainfall and lower river flows from riparian countries. Because agreements on water between riparian countries are either hardly effective or non-existent, there are no guarantees that Iraq will ever receive as much water as before (UN-ESCWA and BGR, 2013; Al-Manmi, 2009). Therefore, it is important for the region to develop sound hydrological models to keep track on the available water resources.

Several hydrologic studies of the region exist (Chenoweth et al., 2011; Kavvas et al., 2011), but they are generally coarse due to the lack of ground truth and do not yield specific information on hydrology and groundwater storages. Mass observations by the Gravity Recovery and Climate Experiment (GRACE), provide a valuable tool to give more insight in the terrestrial water storages and are widely used as a validation of

HESSD
11, 11533–11563, 2014

global hydrologic models like GLDAS, WGHM and GGP (Voss et al., 2013; Werth et al., 2009; Awange et al., 2011; Hinderer et al., 2006; Schmidt et al., 2008; Ngo-Duc et al., 2007; Llubes et al., 2004). For the Euphrates and Tigris region, a comparison between GRACE and the GLDAS model was made by Voss et al. (2013), which showed that the GLDAS model underestimates both yearly and long-term mass variations, most likely because a groundwater component is missing. Therefore, more accurate hydrological models of Northern Iraq are needed, to capture the region's natural groundwater flow and the main hydrological processes.

In this study, a rainfall–runoff model is developed based on the general hydrology and geology of the region using the topo flex approach from Savenije (2010) and Fenicia et al. (2011). Different satellite missions are merged with available ground data to obtain forcing, calibration and validation data for the model (Schmidt et al., 2008; Werth et al., 2009). GRACE data was used for total water mass calculation. TRMM data was used for daily rainfall. MODIS surface reflectance data was used in combination with altimetry data from the Envisat, Jason 1&2 and GFO satellite missions (Crétaux et al., 2011) to find lake mass variations. Local hydrologic and geologic data were obtained during fieldwork in cooperation with local water experts. Obtained data includes discharge data of one of the Tigris river tributaries (Directorate Dokan Dam, unpublished data) and rainfall data from four stations in the region (Meteorological department Kurdistan, unpublished data).

In this paper, a method is presented to determine the contribution of natural water mass variations to the total observed mass signal from GRACE: firstly, the total mass variation in the study area is derived from GRACE using a mascon approach. Secondly, the surface water mass is calculated and subtracted from mass variation observed by GRACE to derive the water mass variation of groundwater and soil moisture. Finally, the natural variation in soil moisture and groundwater mass is calculated using a newly developed rainfall–runoff model and compared with the results derived from GRACE and surface water mass.

HESSD
11, 11533–11563, 2014

2 Study area

Most of Northern Iraq is part of the upstream catchment of the Tigris river, which originates in Turkey and flows in southwestern direction to the Persian gulf. The total yearly flow of the Tigris at Baghdad is about 50 $km^3\,yr^{-1}$. Half of the flow originates from upstream catchments in Turkey and half from tributaries in Northern Iraq (Brooks, 1997; Altinbilek, 2004). Figure 1 gives the elevation map of the total study area, which includes six main tributaries of the Tigris River of which five have headwaters in Turkey or Iran. The figure also presents a map of the mean yearly rainfall rates between 2002 and 2012 based on TRMM 3B42 data (Huffman et al., 2007), which shows the large climatic variations in this area. While the south-western part of the catchment has a desert climate with rainfall rates up to 200 $mm\,yr^{-1}$, the north-eastern part consists of a mountain range with a considerably colder and wetter climate and rainfall rates up to 1000 $mm\,yr^{-1}$. The mountainous region to the north and northeast is the main source of water of the Tigris River and the arid areas in the southwest are totally dependent on upstream river water (Beaumont, 1998; Brooks, 1997). Beside spatial differences in climates, there are also large seasonal and yearly variations in rainfall and temperatures. Almost all rain falls during the winter period between November and March and mean rainfall rates can drop by fifty percent in dry years.

To ensure water supply in the region and generation of hydropower, many larger and smaller dams are currently under construction. Our study area includes the lakes of Mosul, Dukan, Derbendikhan, Adhaim and Hamrin, but also Lake Tharthar, Habbaniyah and Qadisiyah influences the water masses derived from GRACE (Fig. 2). Additionally, two large salt lakes, Urmia and Razzazah, show water level declines over the last decade.

HESSD
11, 11533–11563, 2014

3 Methods

3.1 GRACE mass calculations

During the last years, several methods have been developed to calculate mass change based on GRACE data like (Swenson and Wahr, 2006; Schrama and Wouters, 2011). Most methods comprise different processing steps, mainly to reduce noise, apply geophysical corrections, add consistency and improve the ability of GRACE to see spatial details. For this study a numerical solution of so-called basin functions is used from Schrama et al. (2014), albeit that the method is implemented at a finer resolution so that mass variations can be retrieved in dises with an approximate radius of 1°. This means that the study area is split up in a finite number of basins or mascons, which have only one variable surface water level. Then, using the influence functions of these mascons, the monthly mass variations are derived from the potential coefficient variation obtained from the GRACE GSM information. Although studies use spatial averaging kernels to reduce noise in the signal, such methods were not implemented in this research. The outcome of the mascon inversion method is that a time series of equivalent water height is obtained by mascon. We use the following relation to obtain the total water mass variation over our study area:

$$H_{\mathrm{tot}} = \frac{\sum_{i=1}^{x} H_{\mathrm{m}}^{i} A_{\mathrm{m}}^{i} P_{\mathrm{m}}^{i}}{A_{\mathrm{tot}}}$$

Where H_{m}^{i} is the equivalent water height in a particular mascon, A_{m}^{i} the total area of a mascon, P_{m}^{i} the percentage of the mascon covered by our study area and A_{tot} The total study area.

Figure 2 gives the mascon coverage and the calculation area of about 260 000 km^2 that was used. The study area was chosen based on the following conditions:

- Large lake mass variations at the border area should be avoided. Especially lake Tharthar had to be included in the central area (Fig. 2).

HESSD
11, 11533–11563, 2014

– Boundaries of the study area should preferably coincide with catchment boundaries.

– The study area preferably includes full mascons only.

Most of the conditions given above are met using the proposed area. For lake Razazzah, the most southern lake, and lake Urmia, the most northern lake, correction are made to prevent overestimation of lake mass. This correction was necessary because the lakes are close the borders of our study area. This resulted in a reduction of $\frac{1}{2}$ of the lake mass for Lake Urmia and $\frac{1}{3}$ of the lake mass for lake Razazzah. Note that these two salt lakes mainly contribute to a gradual decrease of lake mass, while other lakes within the catchment boundaries mainly show a sudden decrease during the drought of 2007 till 2009, caused by lake management. Because our focus in this study is mainly on the water mass depletion between 2007 and 2009, water mass variation of the salt lakes is of less importance.

To compare the total water mass variation of the rainfall–runoff model of Northern Iraq with GRACE, the derived GRACE mass was corrected for the extended area to the southwestern desert, which is about 95 000 km^2 of the total 265 000 km^2 of the study area. Because the estimated volume of groundwater pumping is small (30–35 10^{-3} km^3 yr^{-1} UN-ESCWA and BGR, 2013) compared to the total water mass depletion, and recharge and discharge rates of the aquifers are very low in this area, we do not expect significant groundwater variations in this region. Therefore, we assumed that the soil moisture profile from GLDAS (Rodell et al., 2004) can be used as a measure for the total water mass variation in the area. The new GRACE values for Northern Iraq then becomes:

$$H = \frac{H_t A_t - G_d A_d}{A_t - A_d}$$

Where H is the equivalent water height, A is the total area and G is the soil moisture variation in water depth from the GLDAS model. Subscripts t and d indicate total and desert areas.

HESSD
11, 11533–11563, 2014

Finally, the GRACE values have to be corrected for a part of the Urmia catchment in the northeast. This area is about 45 000 km^2. But because the hydrology and rainfall regime of the area are similar to that in Northern Iraq, the total water mass variations are assumed to be similar to these in Northern Iraq. It is likely that this introduces an error in the calculations on a small time scale due to local rainfall events, but on a longer timescale these errors will be minor due the similarities between the regions.

3.2 Derivation of lake mass

The total lake mass variations play an important role in the water balance of the Tigris region (Voss et al., 2013; Longuevergne et al., 2013). To obtain total lake mass contributions in our study area, time series of both lake level and lake area were calculated. The lake levels are derived from satellite altimetry by Crétaux et al. (2011) and USDA/FAS (2013), which includes data from the Envisat, Jason 1&2 and GFO satellite missions. Area calculations were based on MODIS satellite data and SRTM digital elevation maps (DEM), where the reflectance bands were used to detect water and the DEM to distinguish different water bodies. The actual method uses a 250 m × 250 m grid and comprises of three steps: First, the possible extend of the lake was calculated from the DEM using a minimum and maximum elevation. Secondly, the larger lake areas were selected using MODIS reflectance band 5 (1240 nm, 500 m resolution). Finally, the exact lake borders were defined using MODIS reflectance band 2 (858 nm, 250 m resolution).

From the lake level and lake-area time series stage-area curves were created using linear or cubic regression. In Fig. 3, a comparison is given of the derived stage-area curve from our model and a survey done in 2011, which was obtained using sonar by Issa et al. (2013). To decide whether a cubic regression gives a significant improvement, the F test was used for a 95 % interval. Total volume change over time was then derived from the stage-volume curve, which is the integral of the stage-area curve.

HESSD
11, 11533–11563, 2014

3.3 Rainfall–runoff model

In this study, a rainfall–runoff model was used based on the topo flex approach as proposed by Savenije (2010); Fenicia et al. (2011). This resulted in a model structure based on the geology and topography of the five main tributaries of the Tigris river in Northern Iraq (Fig. 5). Figure 4 gives an oversight of the model reservoirs and parameters. The model consists of unsaturated, fast runoff and groundwater reservoirs in three geologic zones in accordance with geologic maps of Stevanovic and Iurkiewicz (2008):

1. Infiltrative or karstified zone: about one third of the surface are of the mountainous zone consists of karstified limestone and is, therefore, highly infiltrative. These limestones have infiltration rates of more than 50 % and transmissitivies ranging from 9 to 8000 $m^2\,day^{-1}$ (Krásný et al., 2006).

2. Non-infiltrative zone: this zone consists of the other mountainous areas, which are characterised by fast runoff due to shallow soil layers, steep slopes and impermeable underlying formations.

3. Alluvial zone: most of the soils in the dry south western part consist of clay and silt sediments. In this region flash floods are common during the scarce rainfall events.

The rainfall–runoff model consists of seven reservoirs, three reservoirs for the unsaturated zone, two for the deep groundwater and two for the fast runoff process, see Fig. 4. A lag function was added to the model to simulate the routing of water through streams and rivers. The fast runoff and deep groundwater reservoirs of the infiltrative and non-infiltrative zones were combined, because the topography and top soils are comparable and share the same underlying aquifers (Krásný et al., 2006). A total number of fourteen parameters were used in the model. The values of model parameters during calibration were restricted to minimum and maximum bounds, to prevent equifinality and ensure realism of the model. The bounds of the slow reservoir runoff fraction were based on spring and river discharge (Ali and Stevanovic, 2010; Stevanovic et al.,

HESSD
11, 11533–11563, 2014

2009; Directorate Dokan Dam, unpublished data) and the bounds of the storage in the unsaturated reservoir were based on insights of local researchers.

Forcing parameters of the rainfall–runoff model are calibrated rainfall data from the TRMM satellite (Huffman et al., 2007) and reference evaporation derived from GLDAS climatic parameters (Rodell et al., 2004; Allen et al., 1998). TRMM data was calibrated by linear regression with monthly precipitation from four gauging stations in Sulaymaniyah, Dokan, Derbendikhan and Penjwen (Almazroui, 2011). Because these stations are relatively close to each other and precipitation rates vary much throughout the region, it was not possible to base the model only on rainfall gauges. Therefore, calibration values were used to calculate distributed daily rainfall from TRMM and were finally corrected with calibrated snowfall and snowmelt values derived from the GLDAS model. While the mountainous region receives up to 1000 mm yr^{-1} rainfall per year on average, it can be about 200 mm yr^{-1} in the lower parts, see Fig. 1. Additionally, the spatial difference in rainfall also varies widely. Therefore, the model was run separately for all 5 tributaries, with different forcing parameters and different total areas for the geologic zones. Meanwhile, the setup and model parameters were kept the same for the models.

3.4 Model calibration

The rainfall–runoff model was calibrated using both GRACE data and river discharge data, using methods similar to Werth et al. (2009). The most convenient way to evaluate the rainfall–runoff model, is to use the discharge from the total study area, which could be derived from the total discharge of the Tigris river in Baghdad minus the discharge entering the study area from Turkey. Unfortunately, this data were not available and most likely have not been measured. Additionally, the discharge at those points is not suitable for rainfall–runoff modelling, because it is strongly influenced by the operation of upstream dams and reservoirs. The only suitable river discharge data we could obtain was for the inflow of Lake Dukan, which is located in the upstream part of the Lesser Zab catchment (see Fig. 5). Therefore, the performance of the model was first

HESSD
11, 11533–11563, 2014

evaluated for this area and then expanded to the whole of Northern Iraq to allow comparison with GRACE. This expansion is possible due to the incorporation of geologic similarities in the region, which means that we can predict the hydrologic behaviour of the total region based on data of the smaller Dukan area.

Model calibration was done using a Monte Carlo simulation with randomly chosen parameter values for every model run within the given parameter bounds. The total discharge for the Dukan area was evaluated by the Nash–Sutcliffe efficiency (NS) for medium and high flows and by the log Nash–Sutcliffe efficiency ($_{\log}$NS) for low flows:

$$\mathrm{NS}_Q = 1 - \frac{\sum_{t=1}^{T}\left(Q_\mathrm{o}^t - Q_\mathrm{m}^t\right)^2}{\sum_{t=1}^{T}\left(Q_\mathrm{o}^t - \overline{Q_\mathrm{o}}\right)^2} \tag{1}$$

$$_{\log}\mathrm{NS}_Q = 1 - \frac{\sum_{t=1}^{T}\left(\log\left(Q_\mathrm{o}^t\right) - \log\left(Q_\mathrm{m}^t\right)\right)^2}{\sum_{t=1}^{T}\left(\log\left(Q_\mathrm{o}^t\right) - \log\left(\overline{Q_\mathrm{o}}\right)\right)^2} \tag{2}$$

Where Q_o represents the observed daily discharges, $\overline{Q_\mathrm{o}}$ is the average observed daily discharge and Q_m the modelled daily discharge. For the model mass performance, only the NS efficiency was used. Figure 6 gives the pareto front for the average NS and logNS of the river discharge and the NS for the water mass. The presented optimal solution was chosen based on the following condition for the period between 2004 and 2012:

$$\max\left(\frac{\mathrm{NS}_Q + {}_{\log}\mathrm{NS}_Q}{2} + \mathrm{NS}_{\mathrm{GRACE}}\right)$$

The uncertainty bounds of the final result are based on the results from other solutions on the pareto front.

HESSD
11, 11533–11563, 2014

4 Results and discussion

4.1 GRACE

Figure 7 shows the resulting GRACE values in terms of equivalent water height (EWH), with an estimated confidence band of 17 mm (Schrama et al., 2007). Water mass depletion between 2007 and 2009 is 130 mm with a SD of 14 mm, based on the average minimum GRACE values during the years before and the years after the drought period during 2007 to 2009. Because from the wet season water mass can vary due to large variations in soil moisture and temporal depression storage, those values are not useful to get an approximation of groundwater and surface water mass depletion. Therefore, yearly minimum values were used, which are least influenced by the yearly hydrological cycle and are the best representation of groundwater and surface water mass variations. Yearly variation is 171 ± 8 mm based on the minimum and maximum values between 2003 and 2011. In the lower graph of Fig. 7, the regional average monthly rainfall is given for the same period to show the relation between GRACE values and rainfall. The periods with more than average rainfall generally coincide with increasing GRACE values as a consequence of accumulation of rainwater in the catchment areas. The drought period between 2007 and 2009 coincides with an overall decrease in water mass, while the water mass is more or less stable during the periods before and after the drought. The magnitude of the yearly variations in water mass coincides with the yearly rainfall sum and are largest before 2007 and smallest during 2007–2009. After 2009, the yearly rainfall amounts have increased but are still relatively low, which coulde be the reason of the persistent low GRACE values in that period.

4.2 Surface water

To compare the total lake mass change with GRACE, all lake volume variations were added up and divided by the total area of the region, resulting in the surface water mass variation in terms of EWH (Fig. 8). The total lake mass accounts for 74 ± 4 mm

HESSD
11, 11533–11563, 2014

of the water mass depletion and 55 ± 5 mm of the yearly water mass variation. This means that more than 50 % of the total water mass depletion is caused by a decline of surface water mass. Such declines in surface water mass were already claimed for the whole Euphrates and Tigris basin by Longuevergne et al. (2013), but their values are higher than those given by Voss et al. (2013). Differences between the results of these researches are likely caused by differences in the size of the studied basins, but exclusion of mostly smaller lakes can also play an important role. For example, lakes Hamrin, Dukan and Mossoul, had a total volume decline of at least 5 km^3 during the study period. The relatively large contribution of those smaller lakes is mainly because the water level variation in those lakes is much larger than the major lakes. The yearly peaks in lake mass lag behind the peaks in GRACE mass, which is because the total water mass increases during winter due to snowfall and rainfall, while it takes time untill this water has been routed to the lakes and reservoirs. The difference in snow and lake mass peaks in Fig. 8 give a good illustration of this process. Snow mass accumulates during winter and almost all snow melts away during spring, feeding the reservoirs in the region. Snow mass values were acquired from GLDAS (Rodell et al., 2004) and show a yearly variation between 11 ±2 and 43 ± 7 mm. Because the snow melts away every spring, snow water mass only influences the yearly water mass variations and does not influence water mass depletion at a longer time scale.

4.3 Natural groundwater variations

The total water mass variations derived from the rainfall–runoff model are given in Fig. 9, together with the contribution of the groundwater, fast runoff and unsaturated reservoirs. Modelled groundwater variations contribute 38 ± 4 mm to the yearly water mass variations and 37 ± 6 mm to the water mass depletion between 2006 and 2009. This is about two third of the total groundwater depletion and at least one fourth of the total water mass depletion. The large contribution of the natural groundwater mass also explains why those values where not reproduced by the GLDAS model, because GLDAS does not include groundwater storage. The time series for the groundwater

HESSD
11, 11533–11563, 2014

reservoir as given in Fig. 9 comprises a period with stable groundwater levels till 2007, followed by a period with groundwater depletion from 2007 till 2009, and a second period with stable groundwater levels from 2010 till 2012. Groundwater from the karstified aquifers plays an important role in the groundwater depletion between 2007 and 2009, because of its high recharge during wet periods and fast discharge through springs during dry periods. While the aquifers still discharge water through springs during dry years, there is much less replenishment of groundwater and groundwater levels will drop. In the governorates of Sulaymaniyah and Duhok alone, about 1.5 $km^3 yr^{-1}$ water emerges every year from springs (Stevanovic and Markovic, 2004; UN-ESCWA and BGR, 2013). After 2009, modelled groundwater levels remained stable because rainfall rates were still below average, but a sequence of years with higher rainfall will likely result in a rise of groundwater levels and a revival of spring discharge.

The unsaturated reservoir shows the same pattern every year, with wet top soils during the rainy season and dry or almost dry conditions during dry periods. The average yearly variation of the unsaturated reservoir is 63 ± 3 mm. The fast runoff reservoir, which represents overland flow and interflow in the basin, shows peaks up to 60 mm during and shortly after intense rainfall events. During the periods with high rainfall, the values are relatively high and decrease fast when the rains end. The average yearly variation of the fast reservoir is 38 ± 2 mm. Both reservoir storages have, therefore, no significant influence on the water mass depletion on the longer term, but have a large contribution to the yearly variation with 100 mm of the total of 170 mm EWH.

4.4 GRACE and modelled values

Figure 9 compares the variation of the total water mass variations in the study area from GRACE and the rainfall–runoff model. The rainfall–runoff model of the entire study area shows an average yearly variation of 138 ± 5 mm and a decline of 34 ± 6 mm between 2007 and 2009. The two graphs differ mainly in the winter and summer peaks. During the wet winter period, patterns are the same, but the amplitudes of the peaks differ, with generally larger peaks in the GRACE data. Possible causes are underestimation

HESSD
11, 11533–11563, 2014

of accumulated snow water or random errors in rainfall rates from TRMM data; these are 23 % on average. Other possible causes are additional water storage in depressions or water mass variability of smaller lakes. In theory, we could have changed the maximum storage of the unsaturated zone to fit the given curves better, but this would create a large difference between the modelled and the literature values. The peaks during summer are also smaller in the model compared to the derived GRACE data. In this case, human water use can play an important role, because local water storage is still used for water supply or agriculture during dry periods, contrary to a natural situation. Another possible cause is the reduced amount of vegetation water during the dry period, but this term is probably negligible.

Figure 10 shows the residuals of the water mass derived from GRACE and of the rainfall–runoff model. Although most of the residuals appear to be random, there is a slight downward trend from 2005 onwards and a stronger increase in the years before. This could indicate groundwater extraction in the region, but also an error in the reduction factors for the mass of lakes Urmia and Razazzah. The fast increase in the years before 2005 is likely caused by the spin-up period of the model. The model has a spin-up period of 7 years, but before 2002 rainfall estimates are unreliable and likely overestimated.

5 Conclusions

5.1 Water masses in Nothern Iraq

The presented approach offers the possibility to quantify the different hydrologic processes in the region as well as to quantify the shares of surface water, soil moisture and groundwater in the total water mass variation. More importantly, the overal model shows the natural groundwater variation in contrast to the total groundwater variation from GRACE data, which gives an indication of the human impact on groundwater in the region. With a depletion of 37 ± 6 mm of equivalent water height, the contribution of

HESSD
11, 11533–11563, 2014

natural varation is about two third of the total groundwater depletion of 56 ± 14 mm. This shows that natural groundwater variation has to be taken into account when GRACE mass values are used to determine overdraft of aquifers.

Especially, in the limestone aquifers of Northern Iraq, strong groundwater variations are common due to extensive karst networks with high transmissivities and infiltration rates, feeding numerous springs in the region. Therefore, overpumping of these aquifers is unlikely, as the groundwater table can vary strongly and the regional water supply is mainly supported by surface water. Additionally, almost all irrigation schemes in those areas are directly linked to large reservoirs.

The dependency of this region on surface water is also reflected by the large water mass variations of the surface water, which contributed about 75 mm out of 130 mm EWH observed by GRACE. With decreasing water availability and increasing water demands from riparian countries in the Tigris river catchment, the need for reliable water management tools is growing, including transboundary models. The developed model helps to give insights in the available water resources and water flows between concerned countries and can be used as a base for water allocation and water agreements. Contrary to other studies like (Chenoweth et al., 2011; Kavvas et al., 2011; Voss et al., 2013), main aquifers and water storages were modelled seperately. Results are, therefore, more useful to water managers. Moreover, the model is based and calibrated on both satellite and in-situ data, which enhances its reliability and predictive power.

5.2 Model structure and input data

This research showed that GRACE can be an important data source in rainfall–runoff models because it gives direct measurements of the total water balance of a larger region. Especially in Northern Iraq, where water resources and data on water resources are scarce, this is valuable information. However, it is not possible to determine what causes the water variations in these regions without additional data on precipitation, geology and river discharges. This data can partly be obtained from satellites, but the use of in-situ data is still of vital importance. In our situation, there was only little data

HESSD
11, 11533–11563, 2014

available, but it could be used for both model structure and calibration. Additionally, knowledge from local water experts and field observations gave important information on governing hydrologic processes.

In our case, the rainfall and discharge stations covered only a part of the region, which resulted in increased model uncertainties. For example, the uncertainties in the total groundwater values are mainly caused by the alluvial groundwater reservoirs, which have only a small contribution to the total flow at lake Dukan. Inclusion of discharge data series from other tributaries would reduce these uncertainties and give a better insight in the spatial variability of the region at the same time. Improvements of the model structure should focus on the spatial variability of input data over the whole of Northern Iraq. Firstly, local rainfall events were spread out due to the current approach, which led to an incorrect division between recharge and fast runoff. Secondly, snowfall and snowmelt are important to calculate both river runoff and total water mass. Therefore, a higher accuracy can be gained by inclusion of a, preferably distributed, snow reservoir in the the rainfall–runoff model. Finally, GRACE mass calculations and reservoir storages inside the study are not directly interchangeable and more advanced methods should be used to account for lake mass variations.

References

Al-Manmi, D. A. M. A.: Sirwan Transboundary River basin management, Tigris and Euphrates transboundary river basin management workshop, SIDA, Stockholm, Sweden, 2009. 11535

Ali, M. H.: Transboundary waterways and streams along the Iraq-Iran border lines . . . the reality and future, Tech. rep., Baghdad University, Baghdad, 2007. 11535

Ali, S. S. and Stevanovic, Z.: Time series analysis of Saraw Springs – SE of Sulaimaniya, Iraqi Kurdistan Region, in: Advances in Research in Karst Media, edited by: Andreo, B., Carrasco, F., Durán, J. J., and LaMoreaux, J. W., Springer, Leipzig, 89–94, doi:10.1007/978-3-642-12486-0, 2010. 11541

HESSD
11, 11533–11563, 2014

Allen, R. G., Pereira, L. S., Raes, D., and Smith, M.: FAO Irrigation and Drainage Paper No. 56, Tech. Rep. 56, FAO, Rome, Italy, available at: http://www.fao.org/docrep/x0490e/x0490e00.htm (last access: 20 December 2013), 1998. 11542

Almazroui, M.: Calibration of TRMM rainfall climatology over Saudi Arabia during 1998–2009, Atmos. Res., 99, 400–414, doi:10.1016/j.atmosres.2010.11.006, 2011. 11542

Altinbilek, D.: Development and management of the Euphrates-Tigris basin, Int. J. Water Resour. D., 20, 15–33, doi:10.1080/07900620310001635584, 2004. 11535, 11537

Altinbilek, H. D.: Water and land resources development in Southeastern Turkey, Int. J. Water Resour. D., 13, 311–332, doi:10.1080/07900629749719, 1997. 11535

Awange, J. L., Fleming, K. M., Kuhn, M., Featherstone, W. E., Heck, B., and Anjasmara, I.: On the suitability of the 4 × 4° GRACE mascon solutions for remote sensing Australian hydrology, Remote Sens. Environ., 115, 864–875, doi:10.1016/j.rse.2010.11.014, 2011. 11536

Beaumont, P.: Restructuring of water usage in the Tigris–Euphrates Basin: the impact of modern water management policies, Middle Eastern Na. Environ., 103, 168–186, 1998. 11535, 11537

Brooks, D. B.: Between the Great Rivers: water in the heart of the Middle East, Int. J. Water Resour. D., 13, 291–310, doi:10.1080/07900629749700, 1997. 11537

Chenoweth, J., Hadjinicolaou, P., Bruggeman, A., Lelieveld, J., Levin, Z., Lange, M. A., Xoplaki, E., and Hadjikakou, M.: Impact of climate change on the water resources of the eastern Mediterranean and Middle East region: modeled 21st century changes and implications, Water Resour. Res., 47, W06506, doi:10.1029/2010WR010269, 2011. 11535, 11548

Crétaux, J.-F., Jelinski, W., Calmant, S., Kouraev, A., Vuglinski, V., Bergé-Nguyen, M., Gennero, M.-C., Nino, F., Abarca Del Rio, R., Cazenave, A., and Maisongrande, P.: SOLS: A lake database to monitor in the Near Real Time water level and storage variations from remote sensing data, Adv. Space Res., 47, 1497–1507, doi:10.1016/j.asr.2011.01.004, 2011. 11536, 11540

Fadhil, A. M.: Drought mapping using geoinformation technology for some sites in the Iraqi Kurdistan region, Int. J. Digital Earth, 4, 239–257, doi:10.1080/17538947.2010.489971, 2011. 11534

Fenicia, F., Kavetski, D., and Savenije, H. H. G.: Elements of a flexible approach for conceptual hydrological modeling: 1. Motivation and theoretical development, Water Resour. Res., 47, W11510, doi:10.1029/2010WR010174, 2011. 11536, 11541

HESSD
11, 11533–11563, 2014

Gibelin, A. and Déqué, M.: Anthropogenic climate change over the Mediterranean region simulated by a global variable resolution model, Clim. Dynam., 20, 327–339, doi:10.1007/s00382-002-0277-1, 2003. 11535

Giorgi, F. and Lionello, P.: Climate change projections for the Mediterranean region, Global Planet. Change, 63, 90–104, doi:10.1016/j.gloplacha.2007.09.005, 2008. 11535

Hinderer, J., Andersen, O., Lemoine, F., Crossley, D., and Boy, J.-P.: Seasonal changes in the European gravity field from GRACE: a comparison with superconducting gravimeters and hydrology model predictions, J. Geodyn., 41, 59–68, doi:10.1016/j.jog.2005.08.037, 2006. 11536

Huffman, G. J., Bolvin, D. T., Nelkin, E. J., Wolff, D. B., Adler, R. F., Gu, G., Hong, Y., Bowman, K. P., and Stocker, E. F.: The TRMM Multisatellite Precipitation Analysis (TMPA): quasi-global, multiyear, combined-sensor precipitation estimates at fine scales, J. Hydrometeorol., 8, 38–55, doi:10.1175/JHM560.1, 2007. 11537, 11542

Issa, I. E., Al-Ansari, N., and Knutsson, S.: Sedimentation and new operational curves for Mosul Dam, Iraq, Hydrolog. Sci. J., 58, 1456–1466, doi:10.1080/02626667.2013.789138, 2013. 11540, 11556

Kavvas, M., Chen, Z., Anderson, M., Ohara, N., Yoon, J., and Xiang, F.: A study of water balances over the Tigris-Euphrates watershed, Phys. Chem. Earth, 36, 197–203, doi:10.1016/j.pce.2010.02.005, 2011. 11535, 11548

Krásný, J., Alsam, S., and Jassim, S. Z.: Hydrogeology, in: Geology of Iraq, 1st Edn., edited by: Jassim, S. Z. and Goff, J. C., Publishers Dolin, Prague, 251–287, 2006. 11541

Llubes, M., Florsch, N., Hinderer, J., Longuevergne, L., and Amalvict, M.: Local hydrology, the global geodynamics project and CHAMP/GRACE perspective: some case studies, J. Geodyn., 38, 355–374, doi:10.1016/j.jog.2004.07.015, 2004. 11536

Longuevergne, L., Wilson, C. R., Scanlon, B. R., and Crétaux, J. F.: GRACE water storage estimates for the Middle East and other regions with significant reservoir and lake storage, Hydrol. Earth Syst. Sci., 17, 4817–4830, doi:10.5194/hess-17-4817-2013, 2013. 11540, 11545

Mariotti, A., Zeng, N., Yoon, J.-H., Artale, V., Navarra, A., Alpert, P., and Li, L. Z. X.: Mediterranean water cycle changes: transition to drier 21st century conditions in observations and CMIP3 simulations, Environ. Res. Lett., 3, 044001, doi:10.1088/1748-9326/3/4/044001, 2008. 11535

HESSD
11, 11533–11563, 2014

McLeman, R. A.: Settlement abandonment in the context of global environmental change, Global Environ. Change, 21, S108–S120, doi:10.1016/j.gloenvcha.2011.08.004, 2011. 11535

Michel, D., Pandya, A., Hasnain, S. I., Sticklor, R., and Panuganti, S.: Water challenges and cooperative response in the Middle East and North Africa, in: US-Islamic World Forum, 11–15, US World Forum Papers, available at: http://www.brookings.edu/~/media/Research/Files/Papers/2012/11/iwfpapers/Waterweb.pdf (last access: 25 March 2014), 2012. 11535

Ngo-Duc, T., Laval, K., Ramillien, G., Polcher, J., and Cazenave, A.: Validation of the land water storage simulated by Organising Carbon and Hydrology in Dynamic Ecosystems (ORCHIDEE) with Gravity Recovery and Climate Experiment (GRACE) data, Water Resour. Res., 43, W04427, doi:10.1029/2006WR004941, 2007. 11536

Rodell, M., Houser, P. R., Jambor, U., Gottschalck, J., Mitchell, K., Meng, C.-J., Arsenault, K., Cosgrove, B., Radakovich, J., Bosilovich, M., Entin, J. K., Walker, J. P., Lohmann, D., and Toll, D.: The global land data assimilation system, B. Am. Meteorol. Soc., 85, 381–394, doi:10.1175/BAMS-85-3-381, 2004. 11539, 11542

Savenije, H. H. G.: HESS opinions "Topography driven conceptual modelling (FLEX-Topo)", Hydrol. Earth Syst. Sci., 14, 2681–2692, doi:10.5194/hess-14-2681-2010, 2010. 11536, 11541

Schmidt, R., Petrovic, S., Güntner, A., Barthelmes, F., Wünsch, J., and Kusche, J.: Periodic components of water storage changes from GRACE and global hydrology models, J. Geophys. Res., 113, B08419, doi:10.1029/2007JB005363, 2008. 11536

Schrama, E. J. O. and Wouters, B.: Revisiting Greenland ice sheet mass loss observed by GRACE, J. Geophys. Res., 116, B02407, doi:10.1029/2009JB006847, 2011. 11538

Schrama, E. J. O., Wouters, B., and Lavallée, D. A.: Signal and noise in Gravity Recovery and Climate Experiment (GRACE) observed surface mass variations, J. Geophys. Res., 112, B08407, doi:10.1029/2006JB004882, 2007. 11544

Schrama, E. J., Wouters, B., and Rietbroek, R.: A mascon approach to assess ice sheet and glacier mass balances and their uncertainties from GRACE data, J. Geophys. Res.-Sol. Ea., 119, 6048–6066, doi:10.1002/2013JB010923, 2014. 11538

Stevanovic, Z. and Iurkiewicz, A.: Groundwater management in northern Iraq, Hydrogeol. J., 17, 367–378, doi:10.1007/s10040-008-0331-0, 2008. 11541, 11558

Stevanovic, Z. and Markovic, M.: Hydrogeology of Northern Iraq, Food and Agriculture Organisation of the United Nations, Rome, 2004. 11546

HESSD
11, 11533–11563, 2014

Stevanovic, Z., Iurkiewicz, A., and Maran, A.: New Insights Into Karst and Caves of Northwestern Zagros Northern Iraq, Acta Carsologica, 38, 83–96, doi:10.1007/978-3-642-12486-0, 2009. 11541

Swenson, S. and Wahr, J.: Post-processing removal of correlated errors in GRACE data, Geophys. Res. Lett., 33, L08402, doi:10.1029/2005GL025285, 2006. 11538

Trigo, R. M., Gouveia, C. M., and Barriopedro, D.: The intense 2007–2009 drought in the fertile crescent: impacts and associated atmospheric circulation, Agr. Forest Meteorol., 150, 1245–1257, doi:10.1016/j.agrformet.2010.05.006, 2010. 11534, 11535

UN-ESCWA and BGR: Inventory of Shared Water Resources in Western Asia, Tech. rep., United Nations Economic ans Social Commission for Western Asia, Bundesanstalt für Geowissenschaften und Rohstoffe, Beirut, available at: http://waterinventory.org/ (last access: 17 January 2014), 2013. 11534, 11535, 11539, 11546

USDA/FAS: Global Reservoirs and Lake Monitor, available at: http://www.pecad.fas.usda.gov/cropexplorer/global_reservoir/ (last access: 28 February 2014), 2013. 11540

Voss, K. A., Famiglietti, J. S., Lo, M., Linage, C., Rodell, M., and Swenson, S. C.: Groundwater depletion in the Middle East from GRACE with implications for transboundary water management in the Tigris-Euphrates-Western Iran region., Water Resour. Res., 49, 904–914, doi:10.1002/wrcr.20078, 2013. 11534, 11536, 11540, 11545, 11548

Werth, S., Güntner, A., Petrovic, S., and Schmidt, R.: Integration of GRACE mass variations into a global hydrological model, Earth Planet. Sc. Lett., 277, 166–173, doi:10.1016/j.epsl.2008.10.021, 2009. 11536, 11542

HESSD
11, 11533–11563, 2014

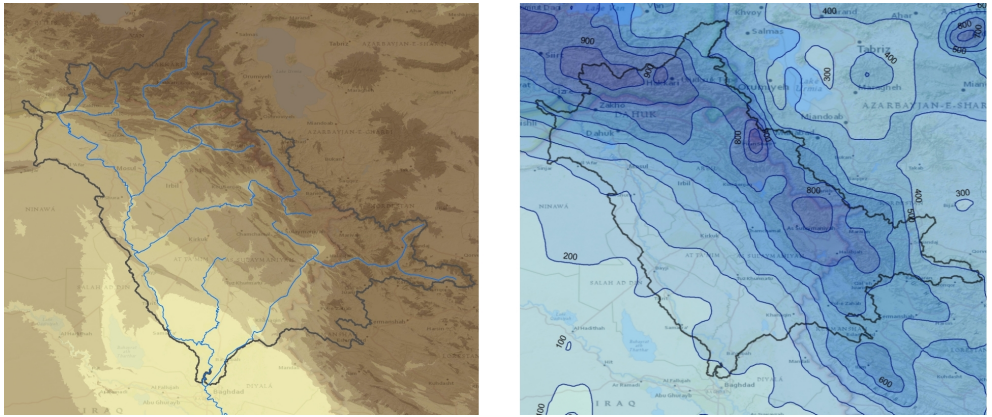

Figure 1. (left) Topographic map of Northern Iraq based on SRTM data and (right) the average yearly rainfall between 2002 and 2012 (mm yr^{-1}) based on TRMM data.

HESSD
11, 11533–11563, 2014

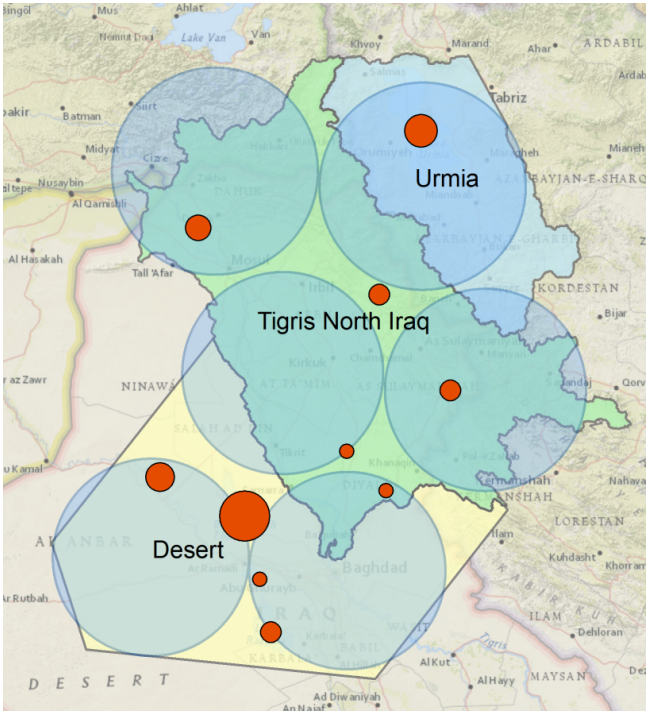

Figure 2. Mascon coverage area for GRACE calculations. In the south-west the included desert area and in the north-east the included Urmia catchment. The larger circles show the coverage of the used mascons and the red dots the location of large lakes and reservoirs in the area. The size of the dots indicates the contribution of different lakes to the total water mass depletion. Lake Tharthar, in the southwestern part, shows the largest water mass depletion.

HESSD
11, 11533–11563, 2014

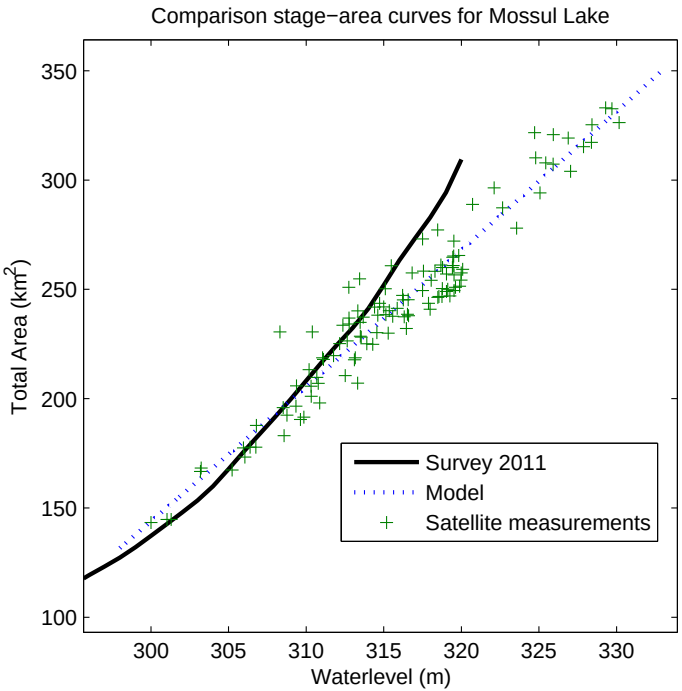

Figure 3. Linear regression stage-area curve for lake Mossul. The curve is compared with a survey in 2011 using sonar by Issa et al. (2013).

HESSD
11, 11533–11563, 2014

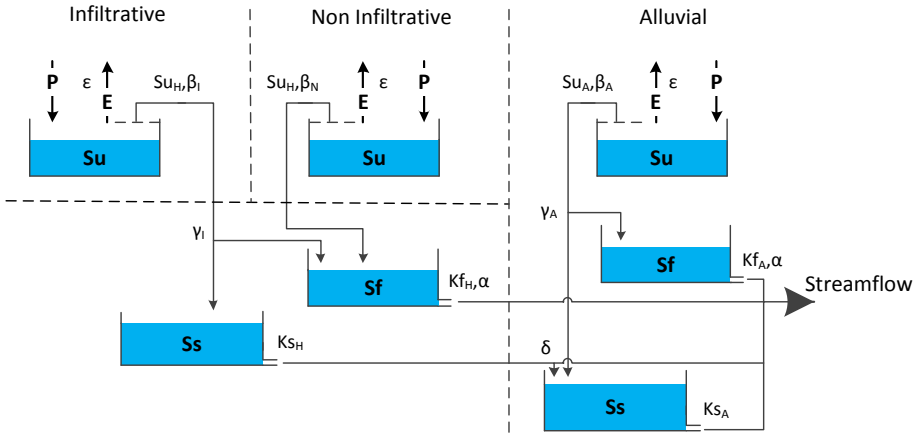

Figure 4. Setup of the rainfall–runoff model based on the three main land classes in Northern Iraq. The upper three reservoirs (Su) represent the water storage in the unsaturated zone, the middle two reservoirs (Sf) represent the water storage related to fast runoff processes, which consist of overland flow and interflow. The two lower reservoirs represent the groundwater storage, which is the main focus in this study. The water fluxes, indicated with arrows, are calculated based on reservoir levels and model parameters.

HESSD
11, 11533–11563, 2014

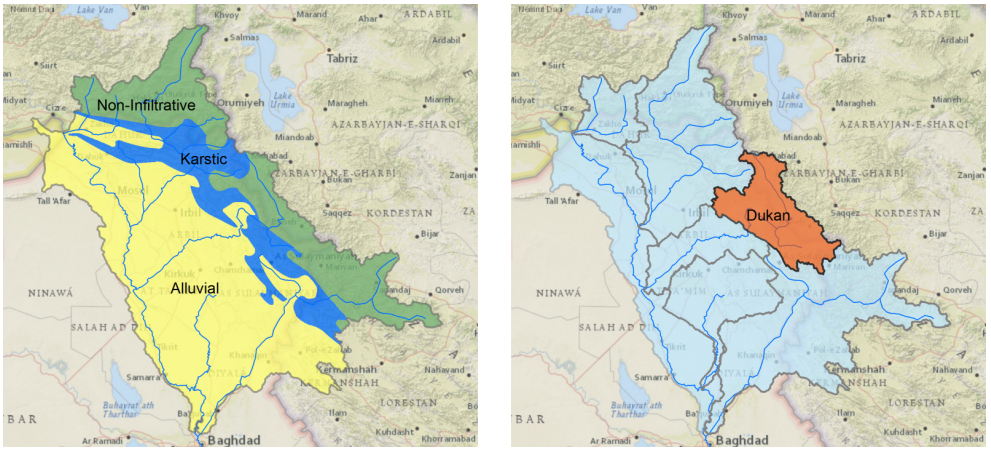

Figure 5. (left) Approximate division of Northern Iraq into three geologic zones, mainly based on (Stevanovic and Iurkiewicz, 2008). (right) Boundaries of main tributaries of the Tigris in Northern Iraq with the Dukan area given in red. Calibration on streamflow is based on measurements from the Dukan area and calibration for water mass is based on the whole Tigris catchment of Northern Iraq.

HESSD
11, 11533–11563, 2014

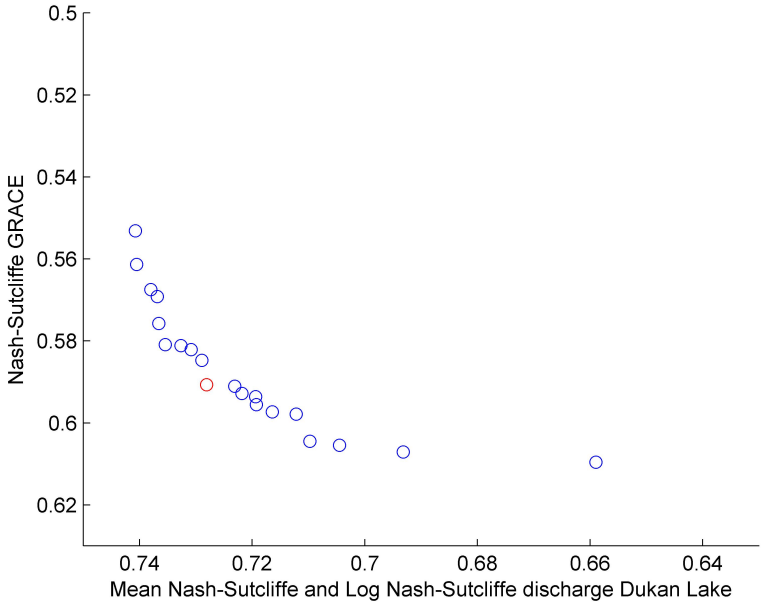

Figure 6. Model performance for river flow and GRACE values for all model runs. On the *y* axis the NS model performance for GRACE mass and on the *x* axis the model performance for the averag NS and logNS model performance for river flow at the inflow of lake Dukan.

HESSD
11, 11533–11563, 2014

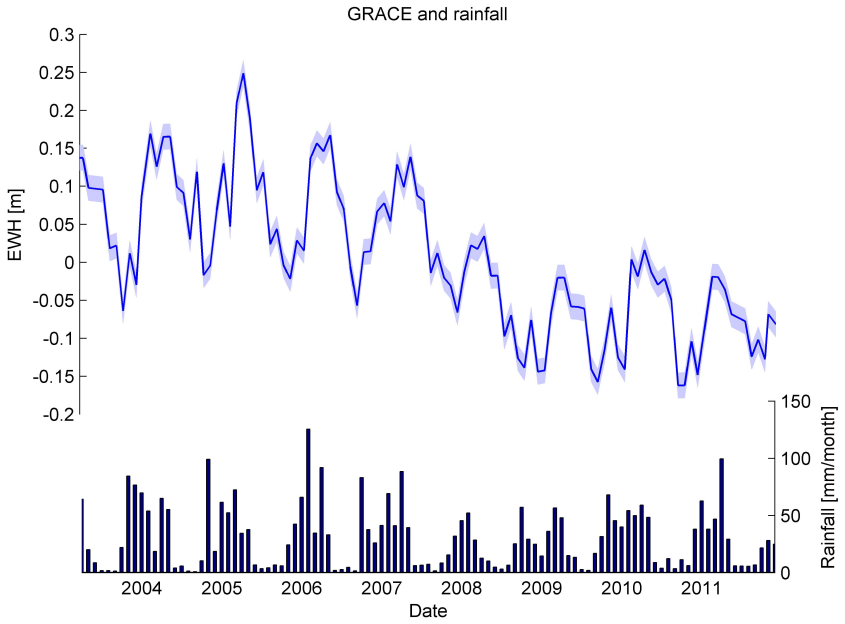

Figure 7. GRACE values and monthly precipitation for extended study area. During the wet winter periods, water accumulates in the region and total water mass increases. Largest water mass depletion occured during seasons of 2007/08 and 2008/09.

HESSD
11, 11533–11563, 2014

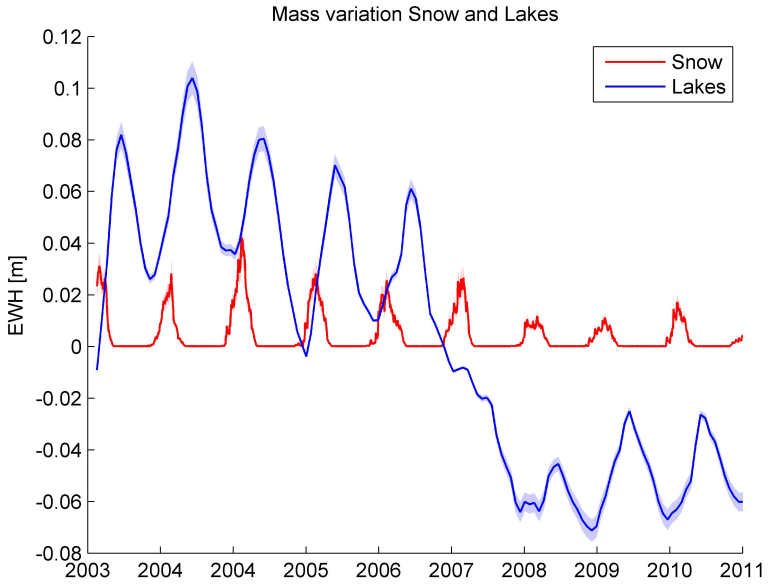

Figure 8. Lake and snow mass for extended study area. Snow accumulates during winter and melts away during spring, while lakes shows the highest water levels at the end of the spring when river discharges drop.

HESSD
11, 11533–11563, 2014

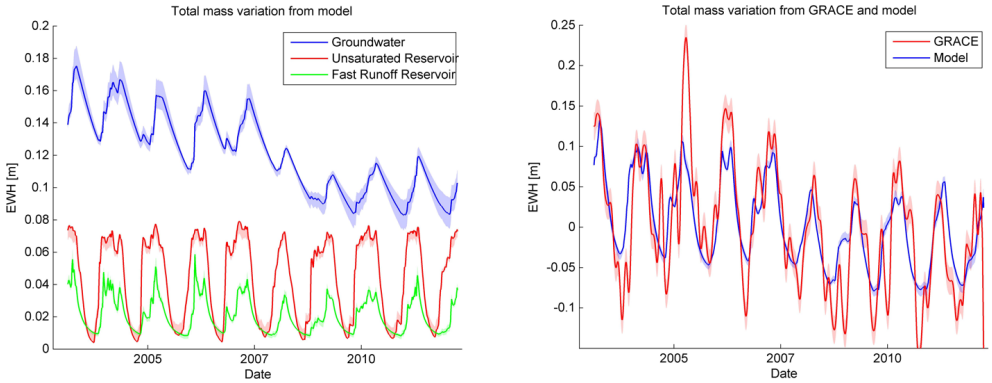

Figure 9. Left: water mass of the different model elements smoothed over 10 days, showing a permanent decline of groundwater and a recurrent pattern for the unsaturated and fast reservoirs. Right: total water mass of GRACE minus surface water mass and the rainfall–runoff model for Northern Iraq.

HESSD
11, 11533–11563, 2014

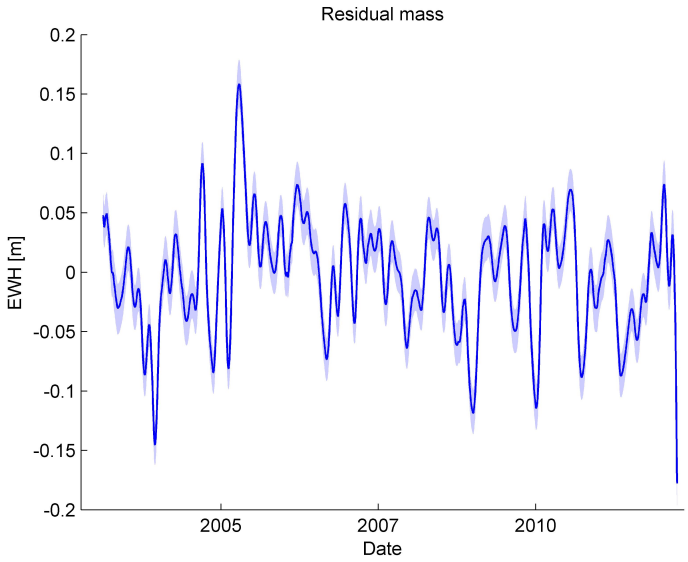

Figure 10. Residual water mass in EWH from the observed GRACE values minus lake mass, snow mass and modelled soil moisture and groundwater mass.

HESSD
11, 11533–11563, 2014